Type II GaSb quantum ring solar cells under concentrated sunlight

Che-Pin Tsai,[1] Shun-Chieh Hsu,[1] Shih-Yen Lin,[2] Ching-Wen Chang,[3] Li-Wei Tu,[3] Kun-Cheng Chen,[4] Tsong-Sheng Lay,[4] and Chien-chung Lin[1,*]

[1]*Institute of Photonic System, College of Photonics, National Chiao Tung University, Tainan, 71150, Taiwan*
[2]*Research Center for Applied Sciences, Academia Sinica, Taipei 11529, Taiwan*
[3]*Department of Physics and Center for Nanoscience and Nanotechnology, National Sun Yat-Sen University, Kaohsiung 80424, Taiwan*
[4]*Department of Electrical Engineering, National Chung Hsing University, Taichung, 402, Taiwan*
[*]*chienchunglin@faculty.nctu.edu.tw*

Abstract: A type II GaSb quantum ring solar cell is fabricated and measured under the concentrated sunlight. The external quantum efficiency confirms the extended absorption from the quantum rings at long wavelength coinciding with the photoluminescence results. The short-circuit current of the quantum ring devices is 5.1% to 9.9% more than the GaAs reference's under various concentrations. While the quantum ring solar cell does not exceed its GaAs counterpart in efficiency under one-sun, the recovery of the open-circuit voltages at higher concentration helps to reverse the situation. A slightly higher efficiency (10.31% vs. 10.29%) is reported for the quantum ring device against the GaAs one.

OCIS codes: (040.5350) Photovoltaic; (350.6050) Solar energy; (250.5590) Quantum-well, -wire and -dot devices.

References and links

1. W. Shockley and H. J. Queisser, "Detailed balance limit of efficiency of p-n junction solar cells," J. Appl. Phys. **32**(3), 510–519 (1961).
2. A. Luque and A. Martí, "Increasing the efficiency of ideal solar cells by photon induced transitions at intermediate levels," Phys. Rev. Lett. **78**(26), 5014–5017 (1997).
3. S. M. Hubbard, C. D. Cress, C. G. Bailey, R. P. Raffaelle, S. G. Bailey, and D. M. Wilt, "Effect of strain compensation on quantum dot enhanced GaAs solar cells," Appl. Phys. Lett. **92**(12), 123512 (2008).
4. R. B. Laghumavarapu, A. Moscho, A. Khoshakhlagh, M. El-Emawy, L. F. Lester, and D. L. Huffaker, "GaSb/GaAs type II quantum dot solar cells for enhanced infrared spectral response," Appl. Phys. Lett. **90**(17), 173125 (2007).
5. P. G. Linares, A. Martí, E. Antolín, C. D. Farmer, Í. Ramiro, C. R. Stanley, and A. Luque, "Voltage recovery in intermediate band solar cells," Sol. Energy Mater. Sol. Cells **98**, 240–244 (2012).
6. C.-C. Lin, M.-H. Tan, C.-P. Tsai, K.-Y. Chuang, and T. S. Lay, "Numerical study of quantum-dot-embedded solar cells," IEEE J. Sel. Top. Quant. **19**, 4000110 (2013).
7. A. Luque, A. Marti, and C. Stanley, "Understanding intermediate-band solar cells," Nat. Photonics **6**(3), 146–152 (2012).
8. N. López, L. A. Reichertz, K. M. Yu, K. Campman, and W. Walukiewicz, "Engineering the Electronic Band Structure for Multiband Solar Cells," Phys. Rev. Lett. **106**(2), 028701 (2011).
9. C. G. Bailey, D. V. Forbes, R. P. Raffaelle, and S. M. Hubbard, "Near 1 V open circuit voltage InAs/GaAs quantum dot solar cells," Appl. Phys. Lett. **98**(16), 163105 (2011).
10. T. Sugaya, O. Numakami, R. Oshima, S. Furue, H. Komaki, T. Amano, K. Matsubara, Y. Okano, and S. Niki, "Ultra-high stacks of InGaAs/GaAs quantum dots for high efficiency solar cells," Energy & Environmental Science **5**(3), 6233–6237 (2012).
11. S. Tomić, A. Marti, E. Antolin, and A. Luque, "On inhibiting Auger intraband relaxation in InAs/GaAs quantum dot intermediate band solar cells," Appl. Phys. Lett. **99**(5), 053504 (2011).
12. P. J. Carrington, M. C. Wagener, J. R. Botha, A. M. Sanchez, and A. Krier, "Enhanced infrared photo-response from GaSb/GaAs quantum ring solar cells," Appl. Phys. Lett. **101**(23), 231101 (2012).
13. T. Tayagaki, N. Usami, P. Wugen, Y. Hoshi, and Y. Kanemitsu, "Enhanced carrier extraction under strong light irradiation in Ge/Si type-II quantum dot solar cells," in *Photovoltaic Specialists Conference (PVSC), 2012 38th IEEE* (IEEE, Austin, TX, 2012), 003200–003203.
14. A. Alemu, J. A. H. Coaquira, and A. Freundlich, "Dependence of device performance on carrier escape sequence in multi-quantum-well p-i-n solar cells," J. Appl. Phys. **99**(8), 084506 (2006).

#201782 - $15.00 USD Received 21 Nov 2013; revised 23 Jan 2014; accepted 4 Feb 2014; published 14 Feb 2014

15. J. Hwang, A. J. Martin, J. M. Millunchick, and J. D. Phillips, "Thermal emission in type-II GaSb/GaAs quantum dots and prospects for intermediate band solar energy conversion," J. Appl. Phys. **111**(7), 074514 (2012).
16. V. Popescu, G. Bester, M. C. Hanna, A. G. Norman, and A. Zunger, "Theoretical and experimental examination of the intermediate-band concept for strain-balanced (In,Ga)As/Ga(As,P) quantum dot solar cells," Phys. Rev. B **78**(20), 205321 (2008).
17. A. Martí, E. Antolín, E. Cánovas, N. López, P. G. Linares, A. Luque, C. R. Stanley, and C. D. Farmer, "Elements of the design and analysis of quantum-dot intermediate band solar cells," Thin Solid Films **516**(20), 6716–6722 (2008).
18. N. Ahsan, N. Miyashita, M. M. Islam, K. M. Yu, W. Walukiewicz, and Y. Okada, "Two-photon excitation in an intermediate band solar cell structure," Appl. Phys. Lett. **100**(17), 172111 (2012).
19. S. M. Hubbard, C. G. Bailey, R. Aguinaldo, S. Polly, D. V. Forbes, and R. P. Raffaelle, "Characterization of quantum dot enhanced solar cells for concentrator photovoltaics," in *Photovoltaic Specialists Conference (PVSC), 2009 34th IEEE*(IEEE, Philadelphia, PA, 2009), pp. 000090–000095.
20. K. Yoshida, Y. Okada, and N. Sano, "Device simulation of intermediate band solar cells: Effects of doping and concentration," J. Appl. Phys. **112**, 084510 (2012).
21. W.-H. Lin, K.-W. Wang, S.-W. Chang, M.-H. Shih, and S.-Y. Lin, "Type-II GaSb/GaAs coupled quantum rings: Room-temperature luminescence enhancement and recombination lifetime elongation for device applications," Appl. Phys. Lett. **101**(3), 031906 (2012).
22. W.-H. Lin, M.-Y. Lin, S.-Y. Wu, and S.-Y. Lin, "Room-temperature electro-luminescence of type-II GaSb/GaAs quantum rings," IEEE Photonic Tech. L. **24**(14), 1203–1205 (2012).
23. J. Nelson, *The Physics of Solar Cells* (World Scientific, 2003).
24. T. Brunhes, P. Boucaud, S. Sauvage, F. Aniel, J. M. Lourtioz, C. Hernandez, Y. Campidelli, O. Kermarrec, D. Bensahel, G. Faini, and I. Sagnes, "Electroluminescence of Ge/Si self-assembled quantum dots grown by chemical vapor deposition," Appl. Phys. Lett. **77**(12), 1822–1824 (2000).
25. T. Gu, M. A. El-Emawy, K. Yang, A. Stintz, and L. F. Lester, "Resistance to edge recombination in GaAs-based dots-in-a-well solar cells," Appl. Phys. Lett. **95**(26), 261106 (2009).
26. M. D. Kelzenberg, D. B. Turner-Evans, B. M. Kayes, M. A. Filler, M. C. Putnam, N. S. Lewis, and H. A. Atwater, "Photovoltaic Measurements in Single-Nanowire Silicon Solar Cells," Nano Lett. **8**(2), 710–714 (2008).

1. Introduction

Since last decades, due to the diminishing reserve of fossil fuel and the concerns of global warming, the need to develop alternative energy sources becomes great. Solar energy has been regarded as a promising candidate for this purpose. Among various technologies, the quantum structure based solar cell is one of the most important designs to push the power conversion efficiency (PCE) over the classic Shockley-Queisser limit (SQ limit) [1,2]. The quantum scale structure, such as quantum dots (QDs) or quantum rings (QRs) [3,4], can construct an extra absorptive transition by introducing an intermediate band (IB) within the band gap of the host material. This intermediate band solar cell (IBSC) allows the extra electron-hole pairs generated from the two inter-band transitions [2], and thus the PCE of the device can surpass the SQ limit. However, since its first introduction in 1997, many attempts to realize such designs have been failed due to serious open-circuit voltage (V_{OC}) reduction of the devices. This drop of V_{OC}, accompanied with limited increase of short-circuit current (J_{SC}), is the main culprit that makes the PCEs of quantum structure embedded solar cells falling behind their single band gap counterparts [5,6]. Many possible explanations/solutions have been provided, such as the flatness of the intermediate band [2], the requirement of half-filled intermediate band [7], carrier recombination [5], the electronic isolation of IB [8], etc.. To fulfill these conditions is not a trivial job for the device designer.

Among the proposed quantum structures, type-I QD is one of the most popular choices for the IBSC. Many researches focused on multiple layer stacking and high quantum efficiency have been published previously [9,10]. However, the high non-radiative recombination rate in these type-I QD (such as InAs or InGaAs QDs) is not favorable for the preservation of V_{OC} [11]. To take another path, a type-II GaSb/GaAs QR structure has been proposed and demonstrated in the hope to improve the situation [11–13]. A typical type-II GaSb/GaAs QR band diagram is shown in Fig. 1. The staggered band offset can facilitate the fast extraction of photo-generated electrons while contain the holes in the QR, and this phenomenon has been demonstrated as a favorable scenario for V_{OC} preservation [14]. The weak coupling between major quantum confined states also prevents the generated carriers from the recombination process [15,16]. For GaSb QR structure, the epitaxial layers could have less strain than QD version [12], which can be very beneficial for high number layers of stacking to enhance the

#201782 - $15.00 USD Received 21 Nov 2013; revised 23 Jan 2014; accepted 4 Feb 2014; published 14 Feb 2014

light absorption at long wavelength. Apart from the epitaxial structure concerns, the ambient sunlight spectrum also poses as an important variable for the solar cell operation. While all previous results of GaSb related solar cell were performed under the standard AM1.5G condition, the concentrated sunlight ambient can be a remedy for aforementioned V_{OC} drop issue. The high density of photons could strengthen the absorption transition for the quantum structures, and this idea has been proposed and demonstrated both theoretically [17] and experimentally [5,18,19].

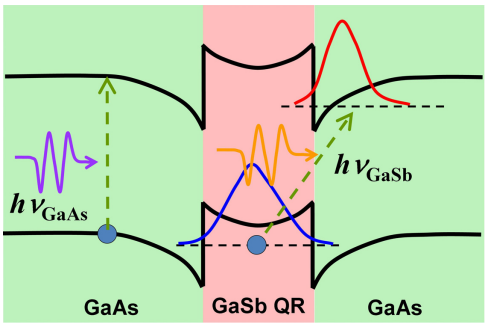

Fig. 1. The band diagram of a GaSb QR in the GaAs material. The electron wavefunction (red) has less overlap with the hole wavefunction (blue), which would be beneficial for less recombination. Two bands of absorption are created: one for GaAs host material ($h\nu_{GaAs}$) and the other for GaSb QR ($h\nu_{GaSb}$), and the latter can effectively increase the photo-current of the device.

In this study, we grow and fabricate a type-II GaSb/GaAs QR structure in a GaAs solar cell device. The room-temperature photoluminescence (PL) shows the high quality of the quantum structure, and the extended long wavelength response of external quantum efficiency (EQE) confirms that the enhanced short circuit current density (J_{SC}) is from these intermediate band absorption. Although the V_{OC} under one sun condition still lags behind the reference sample, the short-circuit current density registers a 7.18% increase compared to reference sample. Under the concentrated sunlight, the recovery of V_{OC} helps to overcome this loss and the higher PCE of the QR cell is observed under 60 sun condition, which agrees with previous prediction [17,20]. The recovery of the V_{OC} can be a good indicator that this type of quantum structure can be useful for the future development of IBSCs.

2. Quantum ring growth and device fabrication

The solar cell wafers were grown in a Riber C21 molecular beam epitaxy (MBE) system and the (100) n-type GaAs substrates were used. Two wafers with and without GaSb QRs were grown and they are referred to as the reference sample and the GaSb QR sample, respectively. The actual epitaxial structures are summarized in Table 1. While the total thickness of the lightly-doped n-type layer is kept the same (1020nm), the QR wafer differs from the reference sample by inserting 3 monolayers (MLs) of GaSb QRs at the center. To have the ring structure instead of dot structure, a post-growth Sb soaking with a specific Sb/As ratio is necessary. The growth procedures and the formation mechanisms of GaSb QRs are discussed elsewhere [21]. By this growth technique, a GaSb QR layer with ring density around 1.9×10^{10} cm^{-2} is obtained for the QR sample discussed in this paper [21]. The average height and outer diameter of rings are 1.5 and 46.7 nm, respectively [21]. Both the reference and the GaSb QR wafers were then went through regular semiconductor process. The p-type metal is Cr/Au and the n-type bottom contact is AuGe/Au, respectively. The H_3PO_4 / H_2O_2 / H_2O solution was used for mesa etch step which defines a 1mm by 1mm square-sized area. The final step is the anti-reflection coating made of SiO_2 100nm to achieve the maximal reception of photons in the visible range.

#201782 - $15.00 USD Received 21 Nov 2013; revised 23 Jan 2014; accepted 4 Feb 2014; published 14 Feb 2014

Table 1. Detailed epitaxial structures of reference and GaSb QR samples

Material		Thickness (nm)		Doping Concentration (cm^{-3})
Ref.	QR	Ref.	QR	
GaAs		200		10^{19}
$Al_{0.8}Ga_{0.2}As$		15		3×10^{18}
GaAs		200		3×10^{18}
GaAs	GaAs	1020	490	2×10^{17}
	(GaAs/GaSb QR 3ML) × 3		10 × 3	
	GaAs		500	
$Al_{0.3}Ga_{0.7}As$		120		3×10^{18}
GaAs		300		3×10^{18}

After the wafer processing, the wafer was cleaved into individual dies and the chip was taken to the regular IV and EQE test under one sun condition. The IV characteristics were taken under the Newport AM1.5G 1000Watts source with Class 1A standard. The currents and voltages were recorded by the HP4156B semiconductor parameter analyzer via a computerized interface. The EQE was taken by Newport 6258 300W Xe lamp with Cornerstone 260 1/4 m monochromator. For the concentration measurement, Keithley 2400 source meter was used to take the IV of the device under test. The concentration was accomplished by a Newport/Oriel 92193 1600Watt Xe lamp with the Newport/Oriel 81030 High Flux Beam Concentrator. All the measurements were performed under a controlled temperature of 25°C.

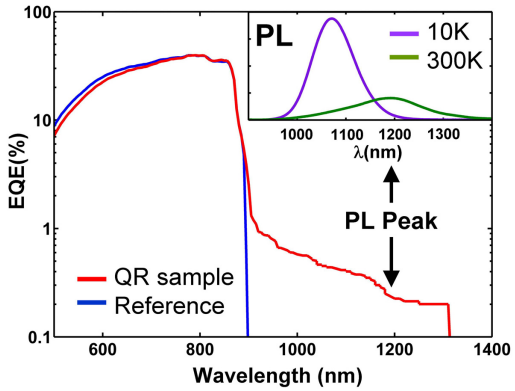

Fig. 2. The EQE spectral response of the reference and GaSb QR samples. The inset is the PL data of the QR under 10K and room temperature.

3. Results and discussion

The PL intensities of the QR sample at low temperature (10K) and room temperature (300K) are shown in the inset of Fig. 2. The wavelengths for peak intensities are at 1072 nm (10K) and 1192 nm (300K), respectively. The full-width-at-half-maximum (FWHM) are 101nm (10K) and 175nm (300K), similar to what we reported before [22].

Figure 2 shows the measured EQE at room temperature. The QR sample has stronger absorption at λ>900nm range, and thus a higher J_{SC}. Compared to the inset PL spectrum, the corresponding peak wavelength falls within the enhanced region of the EQE. Meanwhile, the EQE of the reference GaAs sample falls steeply after 900nm. The one sun IV characteristics is shown in Fig. 3(a). As can be seen from the figure, the one-sun V_{OC} reduction is still severe and the PCE of the QR device suffers from this fact. The short-circuit current, on the other hand, shows considerable enhancement (from 16.84mA/cm^2 to 18.05mA/cm^2, a 7.18%

#201782 - $15.00 USD Received 21 Nov 2013; revised 23 Jan 2014; accepted 4 Feb 2014; published 14 Feb 2014

increase). The PCE of the QR sample is 6.85% while the reference sample is 8.81% under one-sun condition. The lower than average PCE of the reference can be expected from EQE measurement in which the visible wavelength range is not very efficient and the overall peak efficiency is low (about 40%). This is mainly due to non-optimized structure of our design. In fact, we have to compromise our device structure due to epitaxial growth limitation.

The devices were then put under the concentrated sunlight test from 1 sun to 90 sun. An example of concentrated IV curve is shown in Fig. 3(b). The measured PCE, and V_{OC} of the best QR and reference devices under different concentrations are plotted in Fig. 4. From the PCE curve, the QR sample quickly close the performance gap when the pumping intensity goes higher, and eventually surpasses the reference sample at 60 sun test (10.29% vs. 10.31%). The J_{SC} sees a leading edge of QR sample over the whole range of concentration factor. On the V_{OC}, the QR sample outperforms the reference sample at the medium concentration but fall short on the higher intensities. If the fill factor is not considered, and just compare the $J_{SC} \times V_{OC}$ between the QR and the reference samples, a 2% to 7% enhancement can be found under the concentrated sunlight and this ratio is below 1 at one-sun condition.

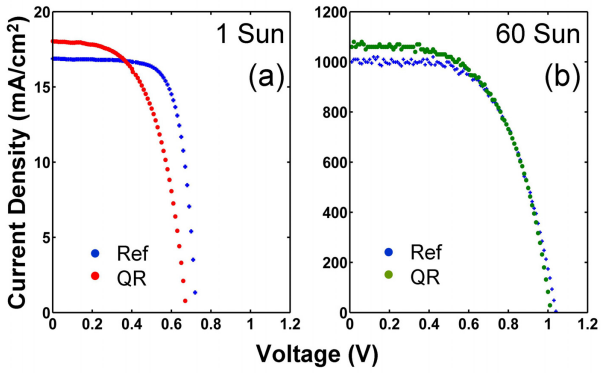

Fig. 3. The current-voltage (IV) characteristics of the reference and GaSb QR samples under (a) one-Sun and (b) 60 Sun.

From previous studies, a two-photon process is needed to fully realize the carrier-generation between the quantum structure levels (QDs or QRs) and the host materials' (such as GaAs) [18]. This two-photon process, however, requires high density of photons to start with from quantum mechanics point of view. So it is natural to see that the efficiency of the QR sample can recover under concentrated light. The behavior of V_{OC} is an indication of the enhanced two-photon transition, which is essential for this type of device to work. However, under the normal one-sun condition, the non-radiative recombination and thermal capture/emission might still be strong enough to offset such two-photon absorption process. To quantitatively evaluate the recombination in our devices, the ideality factor of the diode needs to be acquired. Assuming the current is enhanced by a factor X due to concentration, i. e. $J_{SC}(X) = X \times J_{SC}$. The V_{OC} can be expressed by the following formula [23]:

$$V_{OC}(X) = \frac{nk_BT}{q}\ln\left(\frac{XJ_{SC}}{J_0}+1\right) \approx V_{OC}(1) + \frac{nk_BT}{q}\ln X \begin{pmatrix} 1 & 0 \\ 0 & 1 \end{pmatrix} \qquad (1)$$

, where n is the diode ideality factor, and J_0 is the diode saturation current density. In previous results based on InAs QDs or Si/Ge QDs, the ideality factor of diode can be influenced by the recombination currents of the device. An average value between 1 and 2 can be found in the regular diodes while some could have their ideality factors higher than 2 [3,24]. Even higher ideality factor fluctuation can be found in other cases like nanowire solar cells or devices with strong edge recombination [25,26]. In our devices, the reference GaAs wafer has an ideality

#201782 - $15.00 USD Received 21 Nov 2013; revised 23 Jan 2014; accepted 4 Feb 2014; published 14 Feb 2014

factor of 2.99 across the various concentration condition. The QR samples, on the other hand, have a piecewise linearity of V_{OC} under concentration. On the low concentration, the ideality factor is 3.52, indicating stronger recombination currents in the device. This value drops to 1.3 under higher concentration, which could be viewed as the saturation of the defect-related recombination. Similar slope and piecewise linearity can be observed among the best and typical QR devices, which can be understood as the result of the same epitaxial structure and fabrication processes. Under this condition, the open-circuit voltages at one sun of these devices basically decide how close the QR sample could reach or even surpass the V_{OC} of the reference sample at high concentration of sunlight. The close-in of the V_{OC} in the QR sample agrees well with previous prediction from different groups [17,20], when the concentration factor is properly included in the calculation.

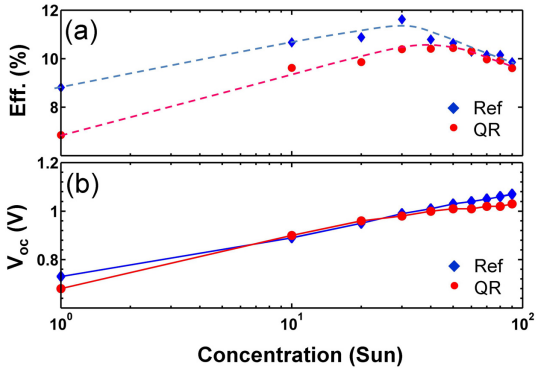

Fig. 4. (a) The power conversion efficiencies of the reference and GaSb QR samples versus different concentration factor. The dashed lines are for eye-guiding only. (b) The V_{OC} under the same condition.

Currently, our devices suffer from the inferior fill factor due to bad series and shunt resistances. Also the overall device structure is not optimized for single junction solar cell due to growth concerns. A switch to metal-organic chemical vapor deposition (MOCVD) growth can possibly solve part of our problems and more cares are necessary to fabricate a high fill factor device in the future. Meanwhile, the QR structure demonstrated its potential to outpace the single band gap device at high concentration and we hope more improvement could lead to its success under one sun condition in the future.

4. Conclusion

In conclusion, we demonstrate a comparison between a single band gap GaAs cell and a type-II GaSb QR solar cell under one sun and concentrated sunlight. The result verifies the theoretical model developed previously. While the device is not optimized for conversion efficiency, the QR sample outperforms its single band gap counterpart at 60-sun illumination condition and the recovery of V_{OC} is observed. We believe the type-II QR structure should be suitable for implementation of the highly efficient IBSC and more studies are underway to improve the device performance in the near future.

Acknowledgments

The authors would like to thank the financial supports from the National Science Council of Taiwan through the grant number: NSC101-2221-E-009-046-MY3.